PAGEOPH, Vol. 135, No. 1 (1991)

0033–4553/91/010031–22$1.50 + 0.20/0

Seismic Tomography Constrained by Bouguer Gravity Anomalies: Applications in Western Washington

J. M. LEES[1] and J. C. VANDECAR[2]

Abstract—Tomographic inversions for velocity variations in western Washington indicate a high correlation with surface geology and geophysical measurements, including gravity observations. By assuming a simple linear relationship between density and velocity (Birch's law) it is possible to calculate the gravity field predicted from the velocity perturbations obtained by local tomographic inversion. While the predicted gravity matches observations in parts of the model, the overall correlation is not satisfactory. In this paper we suggest a method of constraining the tomographic inversion to fit the gravity observations simultaneously with the seismic travel time data. The method is shown to work well with synthetic data in 3 dimensions where the assumption of Birch's law holds strictly. If the sources of the gravity anomalies are assumed to be spatially localized, integration can be carried out over a relatively small volume below the observation points and sparse matrix techniques can be applied. We have applied the constrained inversion method to western Washington using 4,387 shallow earthquakes, to depths of 40.0 km, (36,865 raypaths) covering a 150 × 250 km region and found that the gravitational constraints may be satisfied with minor effect on the degree of misfit to the seismic data.

Key words: Seismic tomography, joint inversion, gravity, regularization, Puget sound, western Washington.

Introduction

The Inversion of geophysical data, particularly seismic data, involves finding a model that predicts a given data set to a given degree of misfit (BACKUS and GILBERT, 1968; CROSSON, 1976; O'SULLIVAN, 1986). Methods for determining three-dimensional velocity models that fit seismic data have been used for over a decade (AKI *et al.*, 1977; SAVINO *et al.*, 1977; CHOU and BOOKER, 1979). With incorporation of computational techniques borrowed from medical imaging (HERMAN, 1980; DINES and LYTLE, 1979; HUMPHREYS *et al.*, 1984; KISSLING *et al.*, 1984; NEUMANN-DENZAU and BEHRENS, 1984), seismic inversion came to be

[1] Institute for Crustal Studies, University of California, Santa Barbara, CA 93106, U.S.A. New Address: Department of Geology and Geophysics, Yale University, 210 Whitney Avenue, New Haven, CT 06511, U.S.A.

[2] Geophysics Program, University of Washington, Seattle, WA 98195, U.S.A.

called seismic tomography, where very large data sets were used to delineate three-dimensional structural details in the crust of the earth. The data sets used in these inversions varied in scope from teleseismic travel times (AKI *et al.*, 1977; SAVINO *et al.*, 1977; HUMPHREYS *et al.*, 1984) to local earthquake travel times (WALCK and CLAYTON, 1987; WALCK, 1988; LEES and CROSSON, 1989) to studies using active sources (IVANSSON, 1986; PAVLIS, 1986; CHIU *et al.*, 1986; EVANS and ZUCCA, 1988). The use of amplitude information from the seismograms was used by HO-LIU *et al.* (1988) and EVANS and ZUCCA (1988) to image the attenuative features of the crust. In most cases resultant images were compared to independent geophysical observations, in part to verify that the tomographic procedures indeed succeeded in imaging believable structures and also to aid interpretation of results. With the advent of more sophisticated computational methods, it becomes desirable to incorporate the comparison of independent observations in the very derivation of the images. LINES *et al.* (1988) have called this approach a "cooperative inversion", where various, potentially different, sets of geophysical observations are brought to bear on the derivation of physically reasonable models. Ultimately, we would expect that all the data, geological and geophysical, should be used in determining structural features of the crust.

LINES *et al.* (1988) have noted that cooperative inversions can be approached either as a joint inversion or as sequential inversion. Joint inversions treat each data set simultaneously: a solution is found which reduces the misfit of each data in some prescribed fashion. The difficulty with joint inversions lies in determining a linear prescription for relating the two independent data sets. Typically this also entails selecting a parameter to represent the relative weights of the data sets. This was the approach taken by JUPP and VOZOFF (1975) to model resistivity and magnetotelluric data. Others have used these techniques to determine joint inversions of velocity and gravity data (SAVINO *et al.*, 1977; RODI *et al.*, 1980; OPPENHEIMER and HERKENHOFF, 1981). Alternatively, sequential inversions treat the data sets separately and relate the inversions by using the results of one inversion as an initial constraint for the others. This approach was taken by LINES *et al.* (1988).

In this paper we follow the simultaneous approach where a joint inversion of local earthquake travel times and gravity observations is calculated. We are primarily concerned with shorter wavelength, local structures where the seismic data offer better resolution, particularly at depth, than the potential field data. The gravity data is thus considered to be a constraint on the seismic data inversion which can be relaxed or strengthened as seen fit. We demonstrate the usefulness of this approach on synthetic data which simulates the characteristics of real earthquake data. Finally, we present the results of the technique applied to a set of 36,865 raypaths in western Washington with a grid of 200 gravity observation points at the surface.

Seismic Inversion

We follow the standard approach used for linearization and discretization that has been applied previously in seismic tomography (AKI *et al.*, 1977; HUMPHREYS *et al.*, 1984; NAKANISHI 1985; HEARN and CLAYTON, 1986; LEES and CROSSON, 1989). In this approach, small perturbations from a one-dimensional, layered background model are derived by assuming a linear relationship between the travel time residuals (Δt) and model parameters (Δs). For a model that is parameterized by small rectilinear blocks this is expressed as a system of linear equations (with n measurements and m unknown model parameters) of the form

$$\mathbf{A}\,\Delta s = \Delta t \tag{1}$$

where $\mathbf{A}$ is an $m \times n$ coefficient matrix (with $A_{ij} = \partial t_i / \partial s_j$ representing the length of the i-th ray in the j-th block), Δs is an m-length vector of slowness perturbations and Δt is an n-length vector of travel time residuals. This system of equations is commonly inconsistent, overdetermined and underconstrained. To eliminate the unconstrained aspect of the problem additional equations are necessary (MENKE, 1984). We follow here the technique of LEES and CROSSON (1989), where the roughness, locally represented as the Laplacian operator, is constrained to be zero within horizontal layers. This requires adding m additional equations to system (1) (one for each model parameter), leading to the modified system

$$\begin{bmatrix} \mathbf{A} \\ \lambda \mathbf{F} \end{bmatrix} \Delta s = \begin{bmatrix} \Delta t \\ 0 \end{bmatrix} \tag{2}$$

where $\mathbf{F}$ represents the Laplacian filter and λ the tradeoff parameter regulating the smoothness of the model versus reduction of misfit to the data.

Gravitational Constraints

In order to incorporate Bouguer gravity data we must assume a relation between velocity (V_p) and density (ρ). The strictest is that of a direct linear relationship with coefficients constant throughout the medium

$$V_p = a + b\rho \Rightarrow \Delta V_p = b\,\Delta\rho \tag{3}$$

where a and b are constants. This approach was introduced by BIRCH (1961) and its applicability is discussed in standard geophysical texts (e.g., STACEY, 1977; MEISSNER, 1986). Since in our inversion procedure we are concerned with slowness, $s = 1/V_p$, rather than velocity, we use the approximate relation

$$\Delta V_p \approx \frac{-1}{s^2}\,\Delta s \tag{4}$$

where s represents background slowness and the relation is valid for small ΔV_p. For an infinitesimal mass anomaly, $dm = \Delta\rho\, dx\, dy\, dz$, located at position $R = (x^2 + y^2 + z^2)^{1/2}$, relative to an observation point at the earth's surface, the vertical component of the observed gravity anomaly is given by

$$dg_z = \Delta\rho G \left(\frac{z\, dx\, dy\, dz}{R^3} \right) \tag{5}$$

where G is the gravitational constant and z is positive downward.

Since each block in our inversion procedure is assumed to have constant slowness (and therefore constant density) the vertical gravitational acceleration, due to perturbations throughout the model, may be simply expressed as a sum over these blocks,

$$\Delta g_z = \int_{\text{model}} dg_z = \sum_j \Delta\rho_j G \int_{\text{block}_j} \left(\frac{z\, dx\, dy\, dz}{R^3} \right). \tag{6}$$

After substituting for $\Delta\rho_j$ from (3) and (4) and rearranging, we arrive at a set of linear equations relating slowness perturbations to observed gravitational acceleration perturbations

$$\Delta g_z^i = \sum_j \left[-\frac{G}{bs_j^2} \int_{\text{block}_j} \left(\frac{z\, dx\, dy\, dz}{R^3} \right) \right] \Delta s_j \quad i = 1, 2, \ldots, n_g \tag{7}$$

where n_g = number of gravitational acceleration observations. Since our observations may be sampled at regular intervals (in our case equal to the horizontal block size) the integral over each block, which represents a geometrical factor, need be calculated only once and kept in a look-up table. Everything within the square brackets may be combined into one term representing the partial derivative of vertical gravitational acceleration perturbation with respect to slowness perturbation. These partial derivatives define the coefficients of a sparse matrix of linear constraints on the model slowness estimate,

$$\Psi_{ij} = -\frac{G}{bs_j^2} \left[\int_{\text{block}_j} \left(\frac{z\, dx\, dy\, dz}{R^3} \right) \right] \tag{8}$$

where the integral over position is relative to observation point i.

If we are concerned mainly with gravity anomalies whose sources lie within the target volume, it is not necessary to integrate over the entire model. The matrix of gravitation constraint equations will then be sparse, as only blocks in the region relatively near the point of measurement need enter the summation of equation (7). This is illustrated in Figure 1, which is a vertical cross section of the three-dimensional model, where each successively lighter shade represents the minimum density perturbation required for a given block to produce a vertical gravity anomaly of at least 1 mgal at the observation point at the surface. This serves to explain why

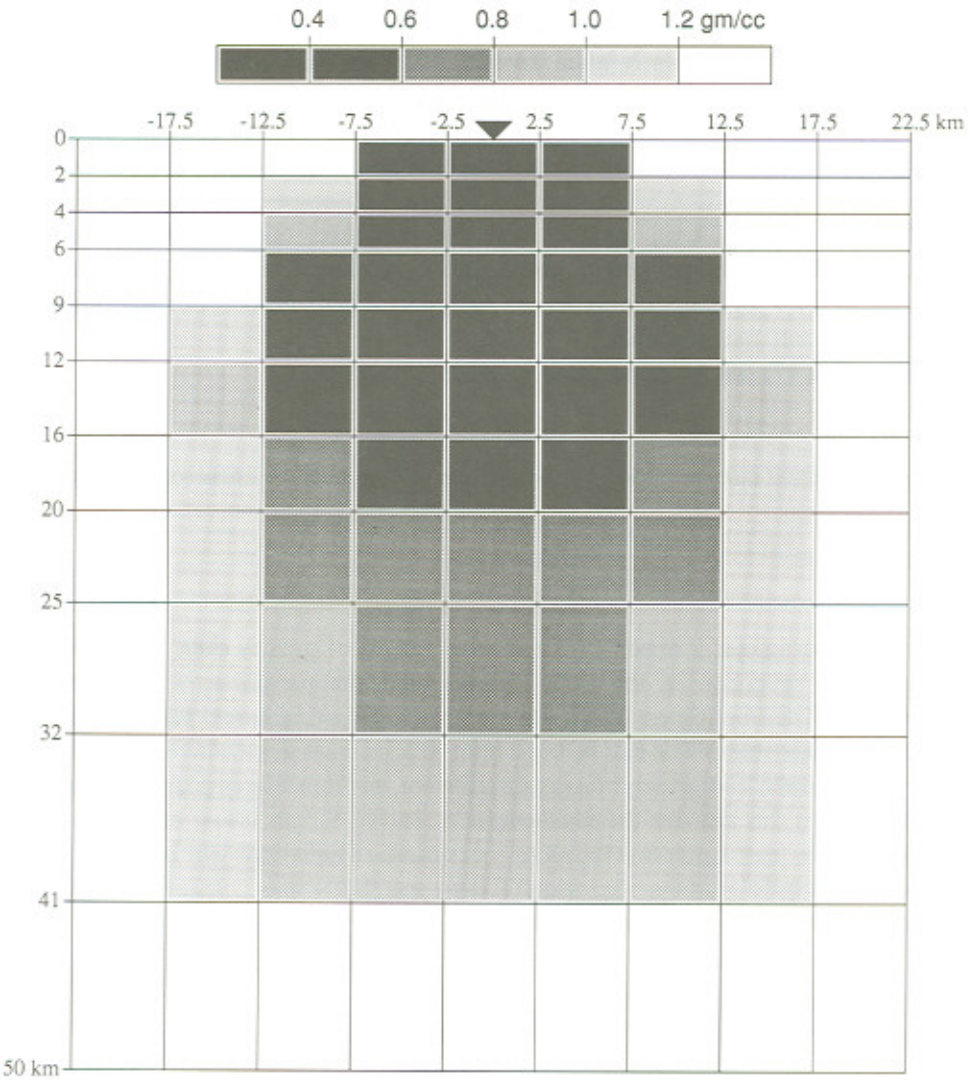

Figure 1

The influence of each block of constant density (and velocity) on the measured vertical gravitational acceleration at the surface point marked by a black triangle. The various shades represent the density anomaly necessary to produce a perturbation of at least 1 mgal. For instance all blocks within the darkest shade require less than a 0.4 gm/cc density anomaly, while the blocks in white require a density anomaly greater than 1.2 gm/cc in order to produce a 1 mgal perturbation. It is therefore the near blocks, as one would intuitively expect, that have the dominant effect on the measurement while blocks at a distance would require unreasonably large anomalies in order to have measurable effect.

shallow layers often dominate the short and middle wavelength features of gravitational inversions, particularly when damping has been introduced. It is all the more pronounced in joint inversions where the seismic data tends to have lower resolution in the shallow regions and therefore is more amenable to changes there. We recognize that spatially extensive density anomalies can give rise to gravity anomalies. But the spatial extent of the gravity anomalies observed in western Washington (half width of 8–12 km), together with the structures observed in the velocity inversions done using no gravity constraints (LEES and CROSSON, 1990), suggest that the sources for these anomalies are indeed localized and that our sparse matrix approach is not unreasonable.

Equation (7) can be represented in matrix form as

$$\Psi \, \Delta s = \Delta g. \tag{9}$$

These equations can be added to the system (2) as a set of linear constraints

$$\begin{bmatrix} \mathbf{A} \\ \lambda \mathbf{F} \\ \gamma \Psi \end{bmatrix} \Delta s = \begin{bmatrix} \Delta t \\ 0 \\ \Delta g \end{bmatrix} \tag{10}$$

where the parameter γ regulates the relative weight of gravity data versus seismic data in the inversion in the same manner that the parameter λ regulates the smoothing. The smoothness constraint requires neighboring model parameters to be related to each other. This can be important in joint inversions where different data sets (e.g., seismic and gravity) constrain different, perhaps nonoverlapping, parts of the model. In this manner the regularization matrix, $\mathbf{F}$, can insure coupling of the data sets. The least squares solution to this system of equations can be found by an efficient conjugate gradient algorithm (PAIGE and SAUNDERS, 1982; SPAKMAN and NOLET, 1988; LEES and CROSSON, 1991).

Simulations

The effectiveness of the technique was demonstrated by generating a simulation inversion with a synthetic model and synthetic data. The perturbation model, consisting of two layers, each with a cross perturbation of +4% and a torus perturbation of −4%, is displayed in Figure 2 (the anomalies have different spatial distributions in each layer). Random sources were distributed throughout the two layers and then connected to a random distribution of 20 stations by calculating raypaths in the layered media. The background reference velocity model and the distribution of raypaths were chosen in a manner simulating actual earthquake data. This model was used to form a set of travel time residuals. Random Gaussian noise was added such that 80% of the root mean square travel time residual was due to noise. To create a set of gravity measurements, a checkerboard grid of

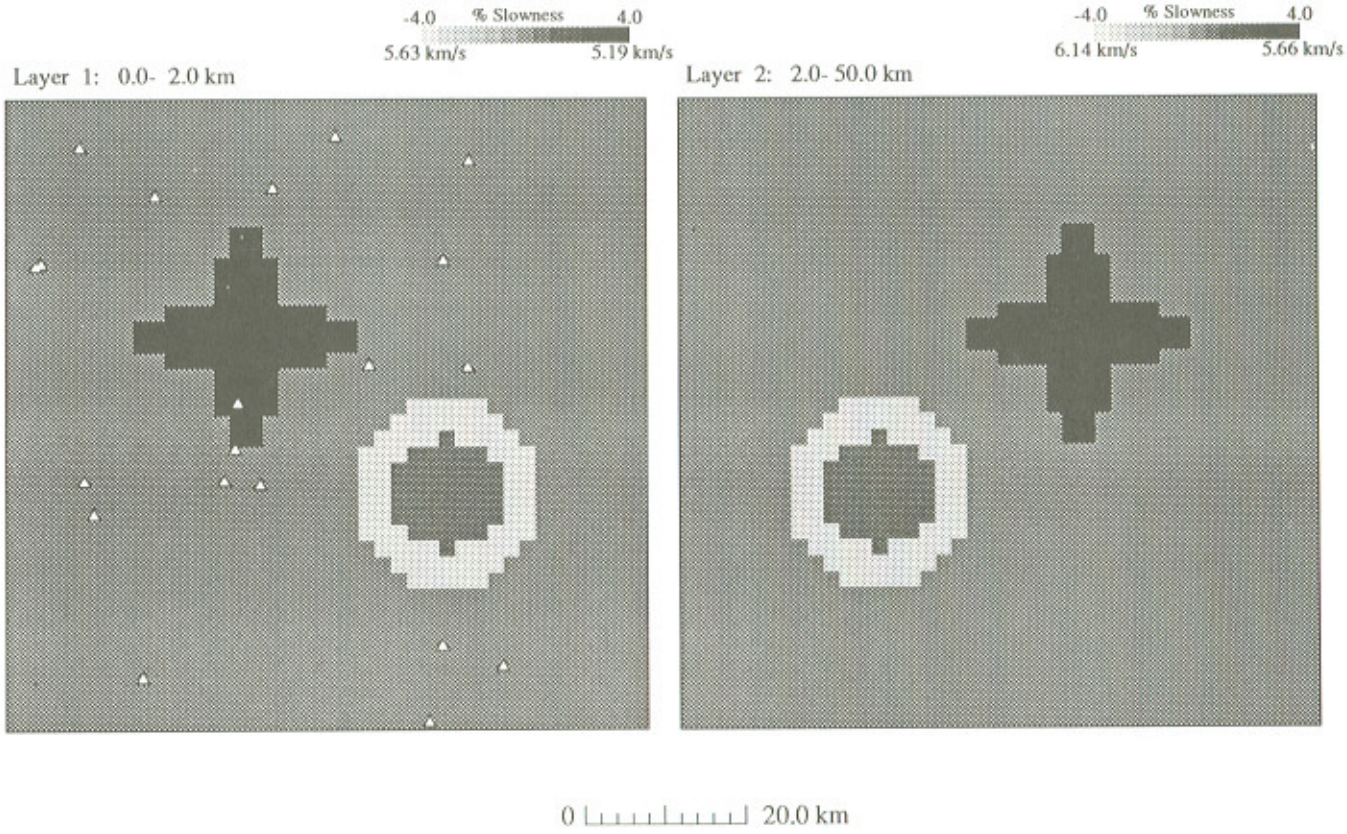

Figure 2
Synthetic model used for inversion simulations Stations, represented as triangles, were distributed randomly at the surface and sources were distributed randomly within the two-layer volume.

measurement points at the surface was fixed and gravity values were determined by integrating the perturbation model according to Equation (7).

First we calculated a solution using no gravity constraints ($\gamma = 0.0$). Damping was found, by trial and error, to have an optimal value of $\lambda = 400$. Additional solutions were produced with this λ fixed while γ was allowed to vary. Results for $\gamma = 0.0, 0.1, 0.5, 1.0$ and 10.0 are displayed in Figure 3. It is clear from this example that the seismic data does not constrain the top layer very well, although the second layer appears to exhibit some of the features of the true anomaly model. As the value of γ is increased the gravity data have more bearing on the inversion and the top layer is better focused. The second layer is improved but to a lesser degree. Beyond some critical value of γ the gravity dominates the inversion and the seismic data has little effect on the outcome producing, due to the smoothness constraints, anomalies smeared into opposing layers. An optimal choice of $\gamma \approx 1.0$, based on various measures of distance from the true model (HERMAN, 1980; LEES and CROSSON, 1991) and on the visual appearance of the images, was determined by trial and error. We are presently investigating the possibility that an optimal choice of γ and λ may be determined through cross-validatory techniques (O'SULLIVAN, 1986; INOUE *et al.*, 1990). In this approach smoothing parameters are determined empirically by excluding portions of the data and inverting the remaining data set, varying a given smoothing parameter. The resulting models are used to predict the travel times of the excluded data. The sum of the squared misfits is used as a summary value, and this value should achieve a minimum for an optimal choice of parameters.

Application to the Puget Sound, Western Washington

We applied these techniques to travel time data in western Washington (LEES, 1989; LEES and CROSSON, 1990). The target region for the Puget Sound inversion is shown in Figure 4 along with the western Washington seismic network stations represented as triangles. The lateral dimensions of the target are 150 km in the east-west direction and 250 km north-south, ranging from 46.4° to 48.5° latitude north and 121.47° to 123.42° longitude west. 4,387 earthquakes were chosen from the western Washington seismic network data-base, including data recorded from 1972 to 1988, resulting in 36,865 raypaths. The target area was divided laterally into blocks 5 km square and 10 layers to a depth of 41 km. The inversion thus required a maximum of 16,000 blocks. While only 10,554 blocks were actually sampled by rays from the selected data, the remaining blocks entered into the solution via the smoothing and gravity constraints. In the center of the model, below 6 km depth, several blocks were sampled by more than 500 rays and the resolution is typically on the order of 3 blocks, or 15 km. Inversion results using only seismic data, equation (2), an extensive interpretive discussion including the geology and error analysis can be found in LEES and CROSSON (1990).

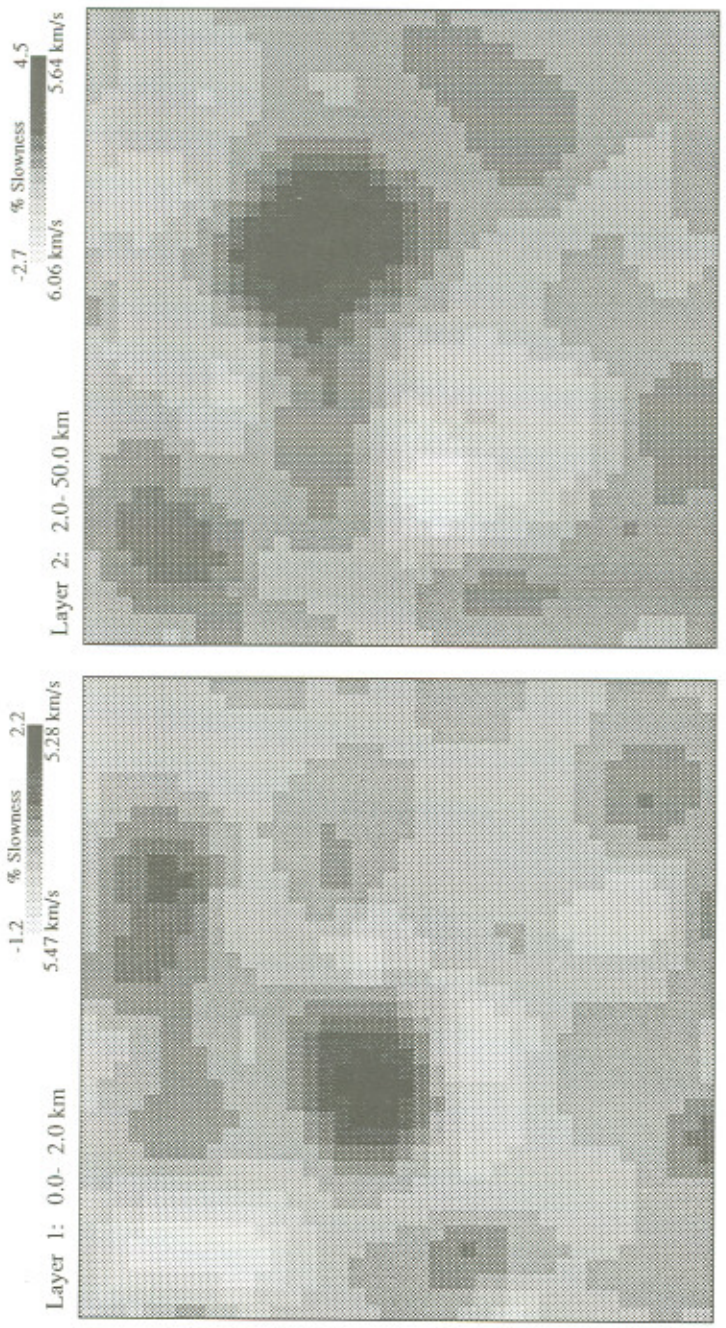
Layer 1: 0.0- 2.0 km
-1.2 % Slowness 2.2
5.47 km/s 5.28 km/s
Layer 2: 2.0- 50.0 km
-2.7 % Slowness 4.5
6.06 km/s 5.64 km/s
0
20.0 km

Figure 3(a)

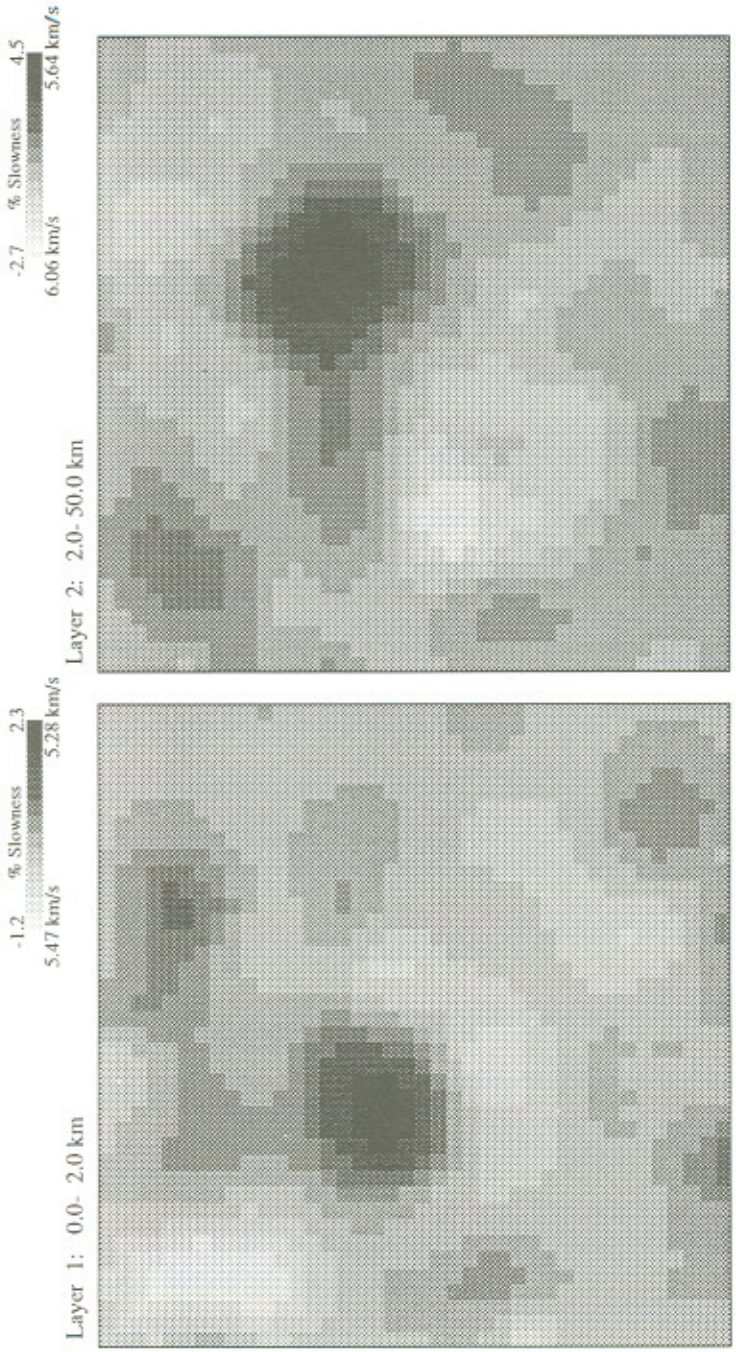
Layer 1: 0.0- 2.0 km
-1.2 % Slowness 2.3
5.47 km/s 5.28 km/s
Layer 2: 2.0- 50.0 km
-2.7 % Slowness 4.5
6.06 km/s 5.64 km/s
0 20.0 km

Figure 3(b)

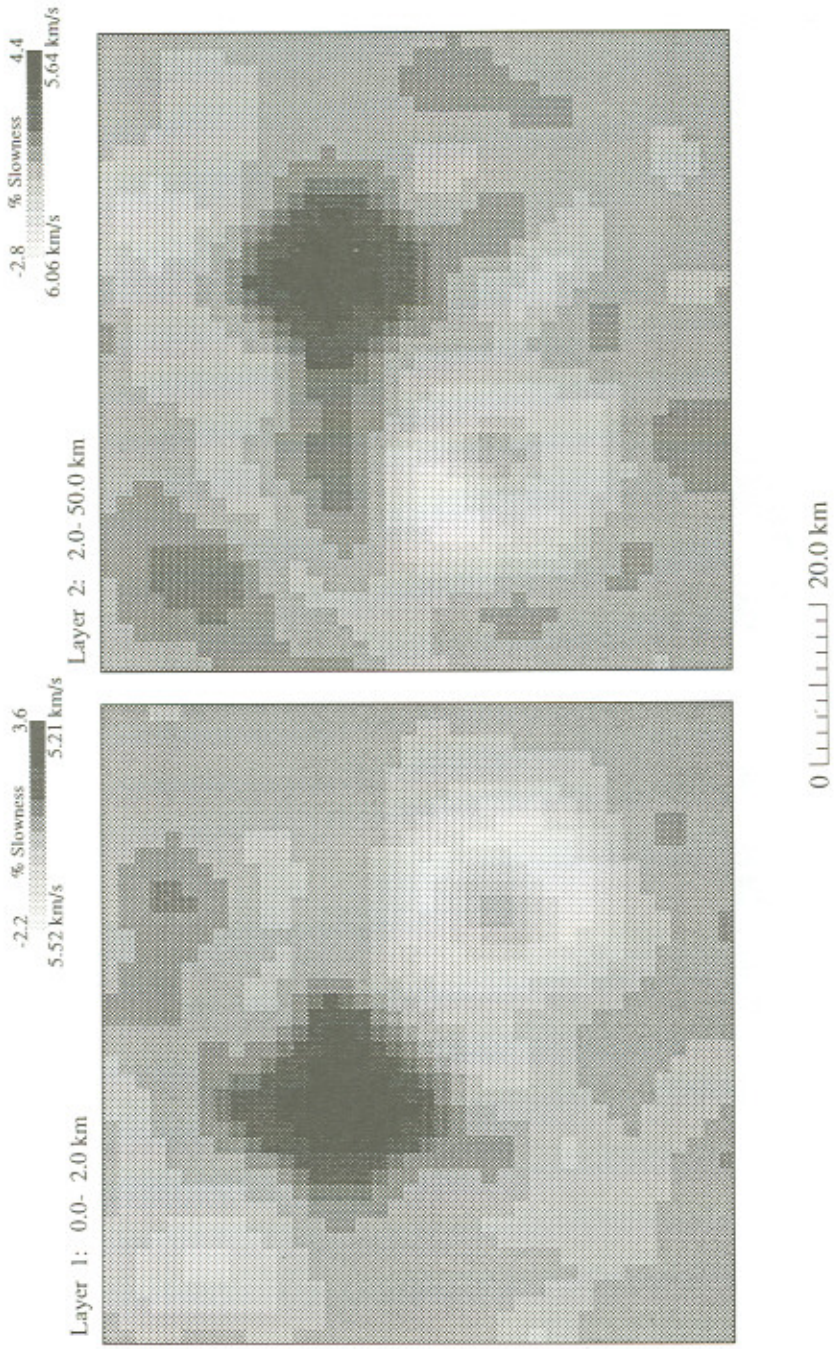
Layer 1: 0.0- 2.0 km
-2.2 % Slowness 3.6
5.52 km/s 5.21 km/s
Layer 2: 2.0- 50.0 km
-2.8 % Slowness 4.4
6.06 km/s 5.64 km/s
0 20.0 km

Figure 3(c)

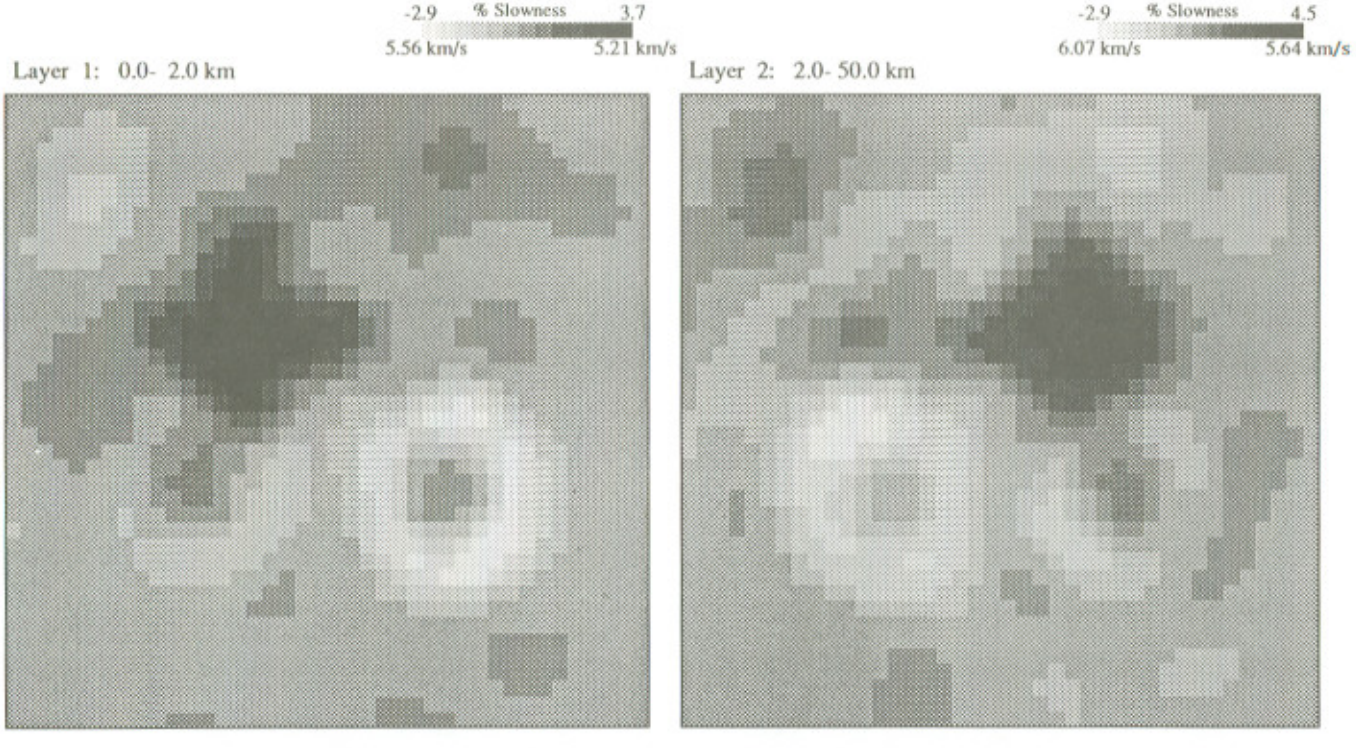
-2.9 % Slowness 3.7
5.56 km/s 5.21 km/s
Layer 1: 0.0- 2.0 km
-2.9 % Slowness 4.5
6.07 km/s 5.64 km/s
Layer 2: 2.0- 50.0 km
0 20.0 km

Figure 3(d)

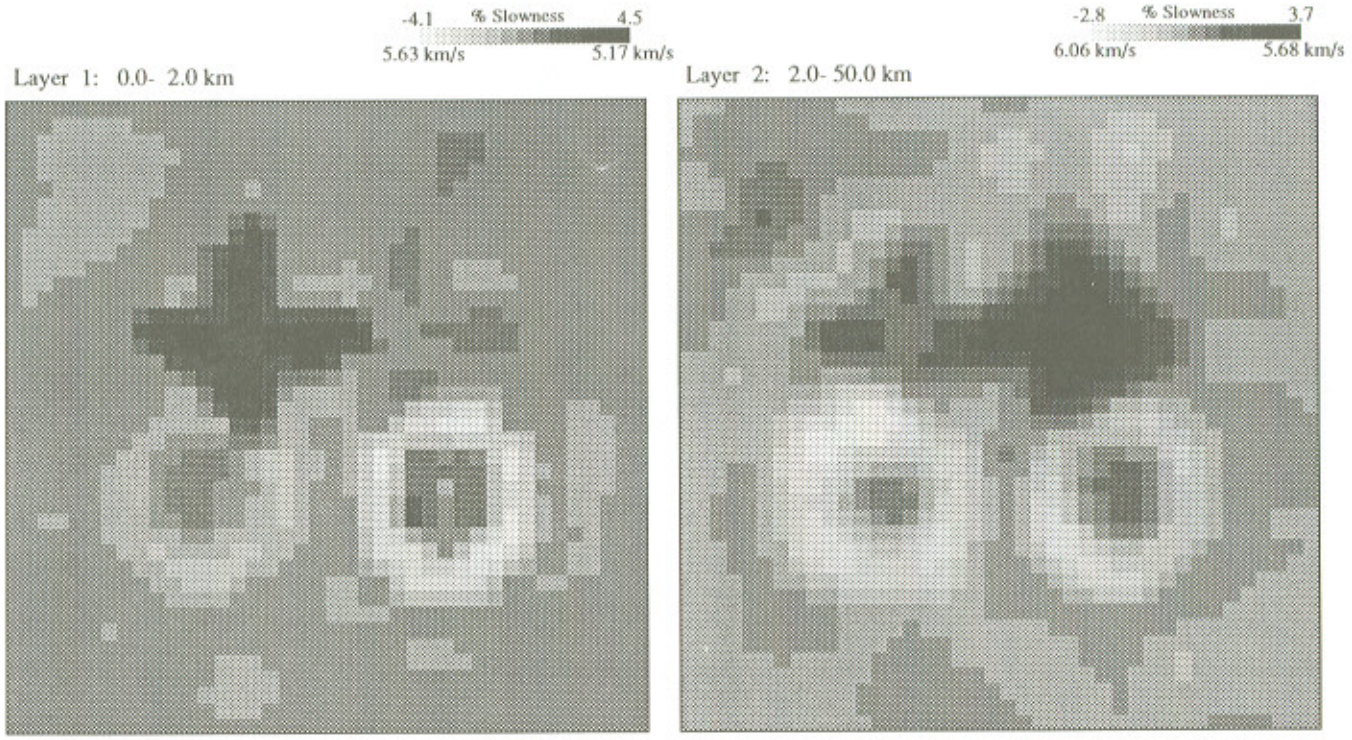

Figure 3(e)
Tomographic inversion of synthetic data using $\lambda = 400$ and a) $\gamma = 0.0$ b) $\gamma = 0.1$ c) $\gamma = 0.5$ d) $\gamma = 1.0$ e) $\gamma = 10.0$.

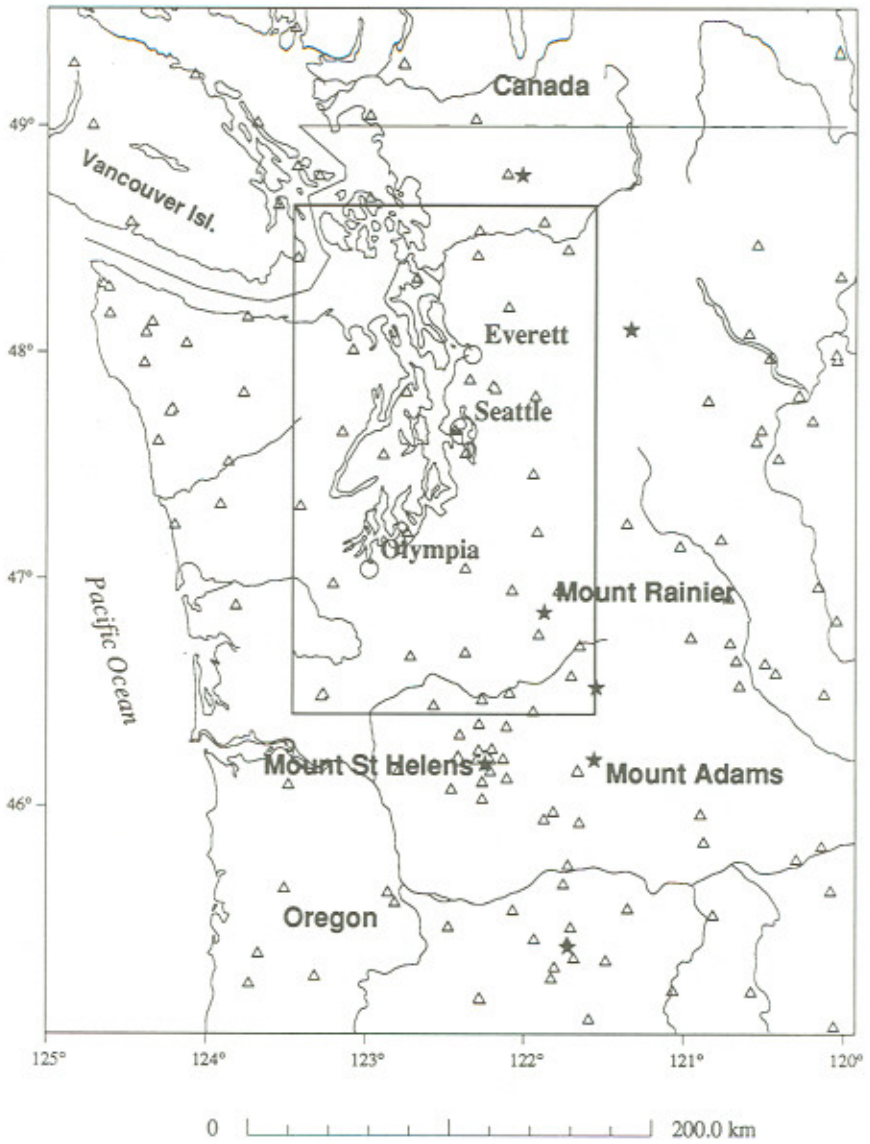

Figure 4
Map of target areas and station distribution of the western Washington seismic network. Triangles are station locations and stars are major strato-volcanos in the region.

In this study we used gravity measurements collected for this region (BONINI *et al.*, 1974) to constrain the inversions according to equation (10). Since we are primarily interested in shorter wavelength structures a linear gradient was removed from the gravity perturbations. Furthermore, we have removed points near the edge of the model so as not to have anomalous features external to the target affecting

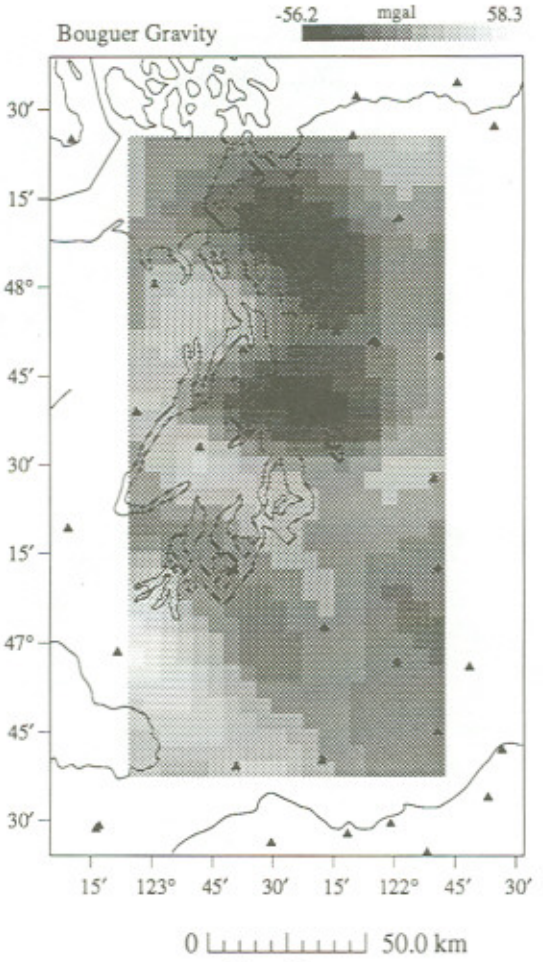

Figure 5
Bouguer gravity anomalies for the Puget Sound region of western Washington.

results internal to the target. The gravity anomalies are displayed in Figure 5. Using the block configuration described in Figure 1 for each gravity observation, and a b value of 2.26 (km/sec)/(g/cm^3) (MEISSNER, 1986), we integrated in three dimensions over a total of 306 blocks down to 32 km depth. Considering that the spatial wavelength of the typical gravity anomaly in western Washington is about 20–30 km, we believe the application of the ideas illustrated in Figure 1 to be conservative and that the sparse matrix approximation is correct.

Results of the inversion with $\lambda = 1000.0$ are displayed in Figures 6a–i ($\gamma = 0.5$) and 7a–c ($\gamma = 0.0$). Notice that in Figure 7 there is some correlation with the gravity in Layer 3 but Layers 1 and 2 show little relation to the gravity fields. It should be stressed that the shallow layers of the inversion are not well constrained

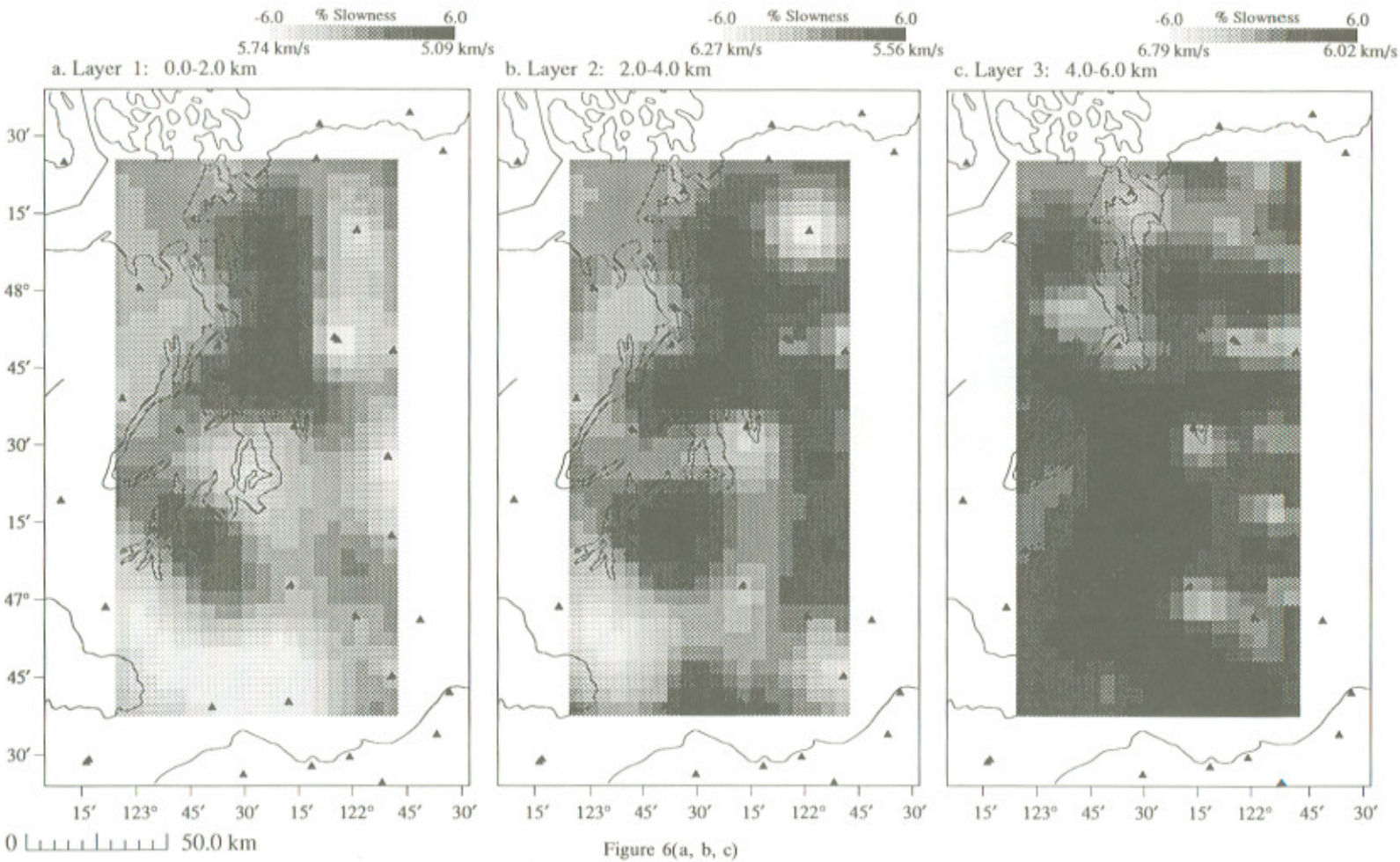
-6.0 % Slowness 6.0
5.74 km/s
5.09 km/s
a. Layer 1: 0.0-2.0 km
-6.0 % Slowness 6.0
6.27 km/s
5.56 km/s
b. Layer 2: 2.0-4.0 km
-6.0 % Slowness 6.0
6.79 km/s
6.02 km/s
c. Layer 3: 4.0-6.0 km
30′
15′
48°
45′
30′
15′
47°
45′
30′
15′ 123° 45′ 30′ 15′ 122° 45′ 30′
0 50.0 km

Figure 6(a, b, c)

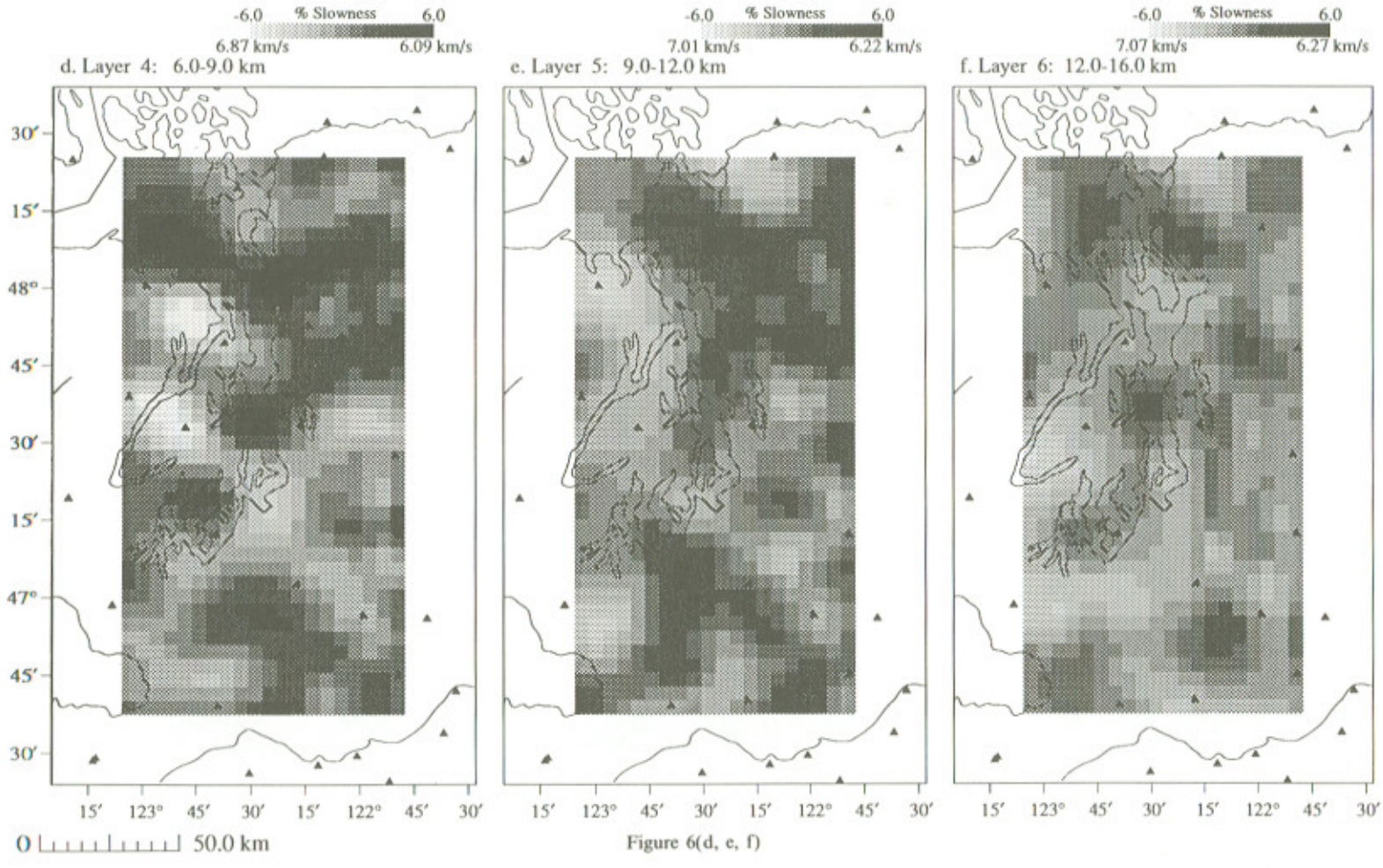
-6.0 % Slowness 6.0
6.87 km/s 6.09 km/s
d. Layer 4: 6.0-9.0 km
-6.0 % Slowness 6.0
7.01 km/s 6.22 km/s
e. Layer 5: 9.0-12.0 km
-6.0 % Slowness 6.0
7.07 km/s 6.27 km/s
f. Layer 6: 12.0-16.0 km
30′
15′
48°
45′
30′
15′
47°
45′
30′
15′ 123° 45′ 30′ 15′ 122° 45′ 30′
0 50.0 km

Figure 6(d, e, f)

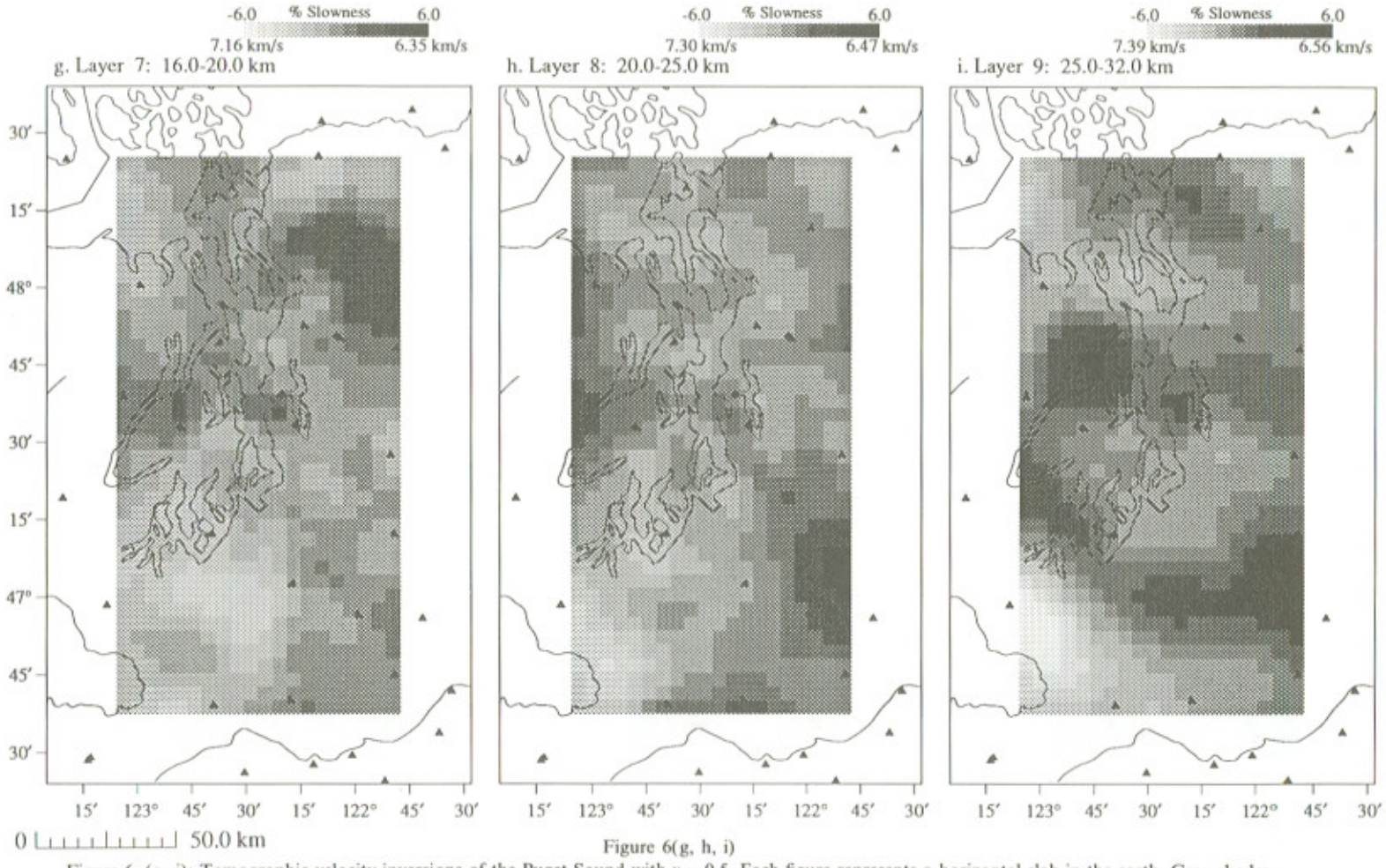

Figure 6(g, h, i)

Figure 6. (a–i): Tomographic velocity inversions of the Puget Sound with $\gamma = 0.5$. Each figure represents a horizontal slab in the earth. Gray shades represent ± 6.0 percent slowness perturbations from the reference model and the corresponding absolute velocities are indicated beneath the scales. Light colored regions are high velocity and dark regions are low velocity. Dark triangles are station locations plotted for reference. The top 2 layers are the most significantly affected by the inclusion of gravity constraints.

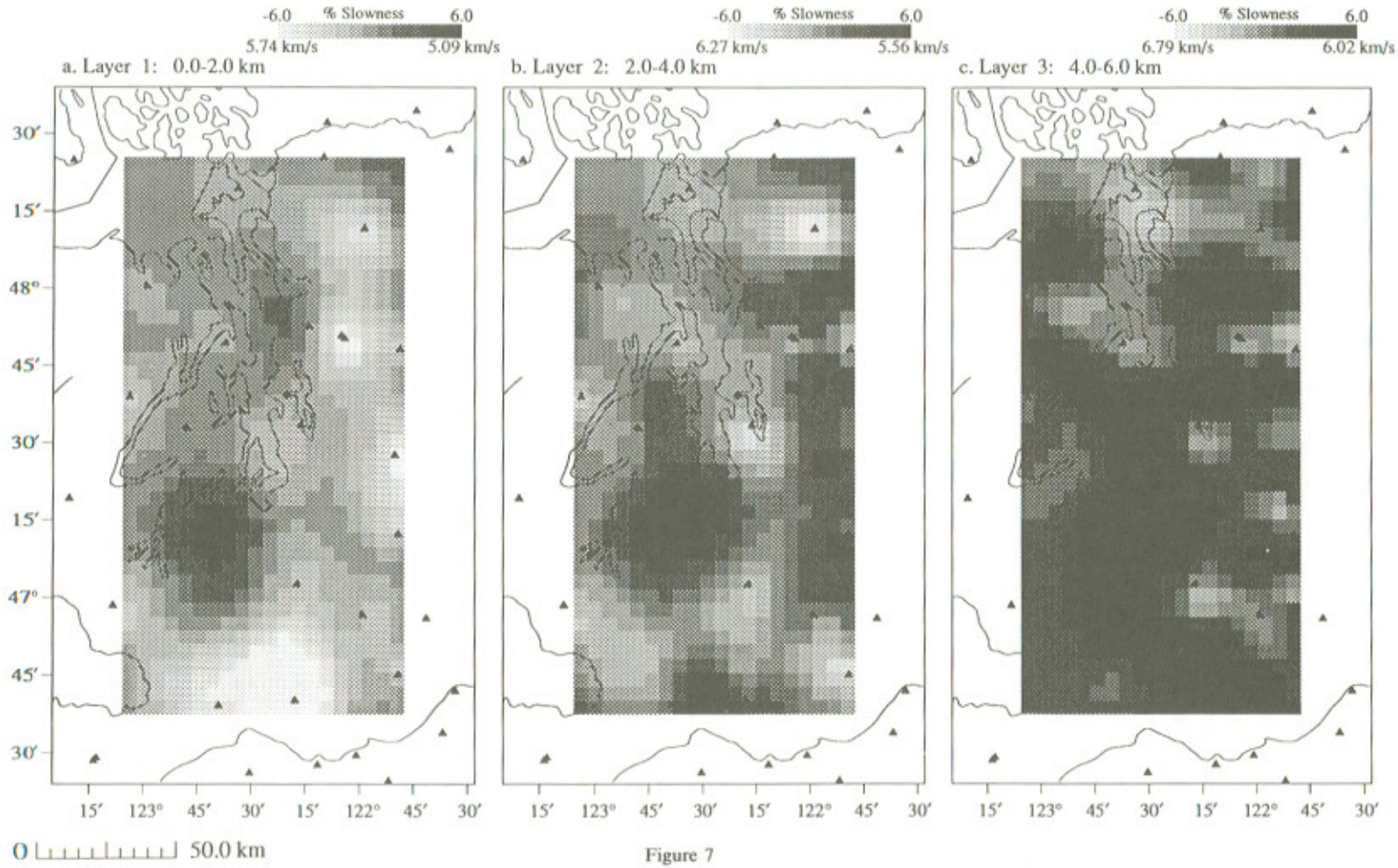

Figure 7

(a–c): Top 3 layers of tomographic velocity inversions of the Puget Sound with $\gamma = 0.0$ to be compared with Figures 6(a–c). A detailed geologic interpretation of the tomographic results is discussed in LEES and CROSSON (1990).

spatially because the seismic rays converge vertically at the surface stations. At lower depths, the seismic data has much better resolution and the influence of the gravity is diminished. The difference in the reduction of misfit (of just the seismic data) between inversions with $\gamma = 0.0$ versus $\gamma = 0.5$ is 0.4% (36.5% versus 36.1%), thus the seismic data has not been significantly compromised by additionally satisfying the gravity data. On the other hand, 90% of the gravity data is explained by the three-dimensional perturbation model. We therefore conclude that the new model satisfies both data sets, at least to the extent determined by the *a priori* choice of smoothing. In this sense we have derived a better or, perhaps, more correct model.

Comparing the inversions with and without gravity constraints we note the two prominent low velocity anomalies near Seattle and Everett in the Puget Sound. While these are evident in Layer 3 of the unconstrained model, they do not appear in the upper two layers (Figure 7). These have been interpreted as deep sedimentary basins controlled by faulting (GOWER *et al.*, 1985; LEES and CROSSON, 1990). In the presence of such strong localized gravity gradients a model with no corresponding, near surface density anomaly would be highly unlikely. The low velocity feature located near Olympia appears on both inversions but note that in the inversion with the gravity constraints it is somewhat better resolved in Layer 1 and a northwest-southeast lineation (observed in Layer 3 of the unconstrained inversion) is enhanced. This linear feature correlates with an observed aeromagnetic anomaly (STANLEY *et al.*, 1987; LEES and CROSSON, 1990). The constrained model therefore agrees better with our *a priori* knowledge of the geology and structure in the region, based on independent information.

Conclusions

We have shown that, given a simple relationship between seismic velocity and density, gravity observations can be simply incorporated in a joint tomographic inversion of travel time data. If we assume that anomalies are localized within the target volume, integration of the model can be restricted and sparse matrix techniques can be employed. By using gravity data as external, *a priori* knowledge we can constrain the model where the seismic data has poor resolution. Smoothing the model insures blending of the data sets and introduces additional *a priori* information regarding the wavelengths of resultant three-dimensional images. In western Washington, the top few layers of the model were most prominently influenced by gravity constraints, the deeper section by the seismic data, and regularization was incorporated by smoothing. Under these conditions, the residual misfit of seismic data was minimally affected, as compared to an inversion without gravity constraints, where as the gravity data was mostly explained by the three-dimensional model, implying that a more appropriate model had been derived. This

also suggests that a simple velocity-density relationship such as Birch's law is probably adequate for western Washington.

Acknowledgements

The authors would like to thank two anonymous reviewers for critical comments that improve this paper. This work was supported by USGS grants 14–08–0001–G1080 and 14–08–0001–G1390.

References

AKI, K., CHRISTOFFERSSON, A., and HUSEBYE, E. S. (1977), *Determination of the Three-dimensional Seismic Structure of the Lithosphere*, J. Geophys. Res. *82*, 277–296.

BIRCH, F. (1961), *The Velocity of Compressional Waves in Rocks to 10 Kilobars, 2*, J. Geophys. Res. *66*, 2199–2224.

BONINI, W. E., HUGHES, D. W., and DANES, Z. F. (1974), *Complete Bouguer Gravity Anomaly Map of Washington*, Washington Division of Geology and Earth Resources, Scale approximately 1:500,000.

BACKUS, G., and GILBERT, G. (1968), *The Resolving Power of Gross Earth Data*, Geophys. J. R. astr. Soc. *266*, 169–205.

CHIU, S. K. L., KANASEWICH, E. R., and PHADKE, S. (1986), *Three-dimensional Determination of Structure and Velocity by Seismic Tomography*, Geophys. *51* (8), 1559–1571.

CHOU, C. W., and BOOKER, J. R. (1979), *A Backus-Gilbert Approach to Inversion of Travel-time Data for Three-dimensional Velocity Structure*, Geophys. J. R. astr. Soc. *59*, 325–344.

CROSSON, R. S. (1976), *Crustal Structure Modelling of Earthquake Data. 1. Simultaneous Least-squares Estimation of Hypocenter and Velocity Parameters*, J. Geophys. Res. *71* (17), 3036–3046.

DINES, K. A., and LYTLE, R. J. (1979), *Computerized Geophysical Tomography*, Proc. IEEE *67*, 1065–1073.

EVANS, J. R., and ZUCCA, J. J. (1988), *Active High-resolution Seismic Tomography of Compressional Wave Velocity and Attenuation Structure at Medicine Lake Volcano, Northern California Cascade Range*, J. Geophys. Res. *93*, 15016–15036.

GOWER, H. D., YOUNT, J. C., and CROSSON, R. S. (1985), *Seismotectonic Map of the Puget Sound Region*, Washington, Map I–1613, U.S. Geol. Survey.

HEARN, T. M., and CLAYTON, R. W. (1986), *Lateral Velocity Variations in Southern California. 1. Results for the Upper Crust from Pg Waves*, Bull. Seismol. Soc. Am. *76* (2), 495–427.

HERMAN, G. T., *Image Reconstructions from Projections* (Academic Press, New York 1980).

HO-LIU, P., KANAMORI, H., and CLAYTON, R. W. (1988), *Applications of Attenuation Tomography to Imperial Valley and Cos-Indian Wells Region, Southern California*, J. Geophys. Res. *93*, 10501–10520.

HUMPHREYS, E., CLAYTON, R. W., and HAGER, B. H. (1984), *A Tomographic Image of Mantle Structure Beneath Southern California*, Geophys. Res. Lett. *11* (7), 625–627.

INOUE, H., FUKAO, Y., TANABE, K., and OGATA, Y. (1990), *Whole Mantle P-wave Travel Time Tomography*, Phys. Earth and Planet. Int. *59*, 294–328.

IVANSSON, S. (1986), *Seismic Borehole Tomography — Theory and Computational Methods*, Proc. IEEE *74*, 2.

JUPP, D. L. B., and VOZOFF, K. (1975), *Stable Iterative Methods for the Inversion of Geophysical Data*, Geophys. J. R. astr. Soc. *42*, 957–976.

KISSLING, E., ELLSWORTH, W. L., and COCKERHAM, R. S. (1984), *Three-dimensional Structure of the Long Valley Caldera, California, Region by Geotomography*, Proc. of Workshop XIX, Active Tectonic and Magmatic Processes beneath Long Valley Caldera, Eastern California, 1, U.S. Geol. Surv. Open File Report, 84–939, 188–220.

LEES, J. M., *Seismic Tomography in Western Washington* (University of Washington, Ph.D. Thesis 1989).

LEES, J. M., and CROSSON, R. S., *Bayesian ART versus conjugate gradient methods in tomographic seismic imaging: An application at Mount St. Helens, Washington*, In *Spatial Statistics and Imaging: Proceedings of the 1988 AMS-IMS-SIAM Summer Research Conference* (ed. Posollo, A.) (in press 1991).

LEES, J. M., and CROSSON, R. S. (1989), *Tomographic Inversion for Three-dimensional Velocity Structure at Mount St. Helens Using Earthquake Data*, J. Geophys. Res. *94* (B5), 5716–5728.

LEES, J. M., and CROSSON, R. S. (1990), *Tomographic Imaging of Local Earthquake Delay Times for Three-dimensional Velocity Variation in Western Washington*, J. Geophys. Res. *95* (B4), 4763–4776.

LINES, L. R., SCHULTZ, A. K., and TREITEL, S. (1988), *Cooperative Inversion of Geophysical Data*, *Geophysics 53* (1), 8–20.

MEISSNER, R., *The Continental Crust: A Geophysical Approach* (Academic Press, Orlando 1986).

MENKE, W., *Geophysical Data Analysis: Discrete Inverse Theory* (Academic Press, Orlando 1984).

NAKANISHI, I. (1985), *Three-dimensional Structure Beneath the Hokkaido-Tohoku Region as Derived from a Tomographic Inversion of P-arrival Times*, J. Phys. Earth *33*, 241–256.

NEUMANN-DENZAU, G., and BEHRENS, J. (1984), *Inversion of Seismic Data Using Tomographical Reconstruction Techniques for Investigations of Laterally Inhomogeneous Media*, Geophys. J. R. astr. Soc. *79*, 305–315.

O'SULLIVAN, F. (1986), *A Statistical Perspective on Ill-posed Inverse Problems*, Stat. Sci. *1* (4), 502–527.

OPPENHEIMER, D. H., and HERKENHOFF, K. E. (1981), *Velocity Density Properties of the Lithosphere from Three-dimensional Modeling at the Geysers-Clear Lake Region, California*, J. Geophys. Res. *86*, 6057–6065.

PAIGE, C. C., and SAUNDERS, M. A. (1982), *LSQR: An Algorithm for Sparse Linear Equations and Sparse Least Squares*, Trans. Math. Software *8*, 43–71.

PAVLIS, G. L. (1986), *Geotomography Using Refraction Fan Shots*, J. Geophys. Res. *91*, 6522–6534.

RODI, W. L., JORDAN, T. H., MASSO, J. F., and SAVINO, J. M. (1980), *Determination of the Three-dimensional Structure of the Eastern Washington from the Joint Inversion of Gravity and Earthquake Travel Time Data*, Final Tech. Rep. SSS–R–80–4516, Systems, Science and Software, La Jolla, California.

SAVINO, J. M., RODI, W. L., GOFF, R. C., JORDAN, T. H., ALEXANDER, J. H., and LAMBERT, D. G. (1977), *Inversion of Combined Geophysical Data for Determination of Structure Beneath the Imperial Valley Geothermal Region.*, Final Tech. Rep. SSS–R–78–3412 to the Department of Energy, Systems, Science and Software, La Jolla, California.

SPAKMAN, W., and NOLET, G., *Imaging algorithms, accuracy and resolution in delay time tomography*, In *Mathematical Geophysics* (ed. Vlaar, N. J.) (D. Reidel Publishing Co. 1988) pp. 155–187.

STACEY, F. D., *Physics of the Earth* (John Wiley & Sons, Inc., New York 1977).

STANLEY, W. D., FINN, C., and PLESHA, J. L. (1987), *Tectonics and Conductivity Structures in the Southern Washington Cascades*, J. Geophys. Res. *92*, 10,179–10,193.

WALCK, M. C. (1988), *Three-dimensional V_p/V_s Variations for the Coso Region, California*, J. Geophys. Res. *93*, 2047–2052.

WALCK, M. C., and CLAYTON, R. W. (1987), *P Wave Velocity Variations for the Coso Region, California, Derived from Local Earthquake Travel Times*, J. Geophys. Res. *92*, 393–405.

(Received January 3, 1990, revised July 29, 1990, accepted October 1, 1990)